Designation: E 2059 – 00a

Standard Practice for Application and Analysis of Nuclear Research Emulsions for Fast Neutron Dosimetry[1]

This standard is issued under the fixed designation E 2059; the number immediately following the designation indicates the year of original adoption or, in the case of revision, the year of last revision. A number in parentheses indicates the year of last reapproval. A superscript epsilon (ϵ) indicates an editorial change since the last revision or reapproval.

1. Scope

1.1 Nuclear Research Emulsions (NRE) have a long and illustrious history of applications in the physical sciences, earth sciences and biological sciences **(1,2)**[2]. In the physical sciences, NRE experiments have led to many fundamental discoveries in such diverse disciplines as nuclear physics, cosmic ray physics and high energy physics. In the applied physical sciences, NRE have been used in neutron physics experiments in both fission and fusion reactor environments **(3-6)**. Numerous NRE neutron experiments can be found in other applied disciplines, such as nuclear engineering, environmental monitoring and health physics. Given the breadth of NRE applications, there exist many textbooks and handbooks that provide considerable detail on the techniques used in the NRE method. As a consequence, this practice will be restricted to the application of the NRE method for neutron measurements in reactor physics and nuclear engineering with particular emphasis on neutron dosimetry in benchmark fields (see Matrix E 706).

1.2 NRE are passive detectors and provide time integrated reaction rates. As a consequence, NRE provide fluence measurements without the need for time-dependent corrections, such as arise with radiometric (RM) dosimeters (see Test Method E 1005). NRE provide permanent records, so that optical microscopy observations can be carried out anytime after exposure. If necessary, NRE measurements can be repeated at any time to examine questionable data or to obtain refined results.

1.3 Since NRE measurements are conducted with optical microscopes, high spatial resolution is afforded for fine structure experiments. The attribute of high spatial resolution can also be used to determine information on the angular anisotropy of the in-situ neutron field **(4,5,7)**. It is not possible for active detectors to provide such data because of in-situ perturbations and finite-size effects (see Section 11).

1.4 The existence of hydrogen as a major constituent of NRE affords neutron detection through neutron scattering on hydrogen, that is, the well known (n,p) reaction. NRE measurements in low power reactor environments have been predominantly based on this (*n,p*) reaction. NRE have also been used to measure the ^{6}Li (*n,t*) ^{4}He and the ^{10}B (*n*,α) ^{7}Li reactions by including ^{6}Li and ^{10}B in glass specks near the mid-plane of the NRE **(8,9)**. Use of these two reactions does not provide the general advantages of the (*n,p*) reaction for neutron dosimetry in low power reactor environments (see Section 4). As a consequence, this standard will be restricted to the use of the (n,p) reaction for neutron dosimetry in low power reactor environments.

1.5 *Limitations*—The NRE method possesses three major limitations for applicability in low power reactor environments.

1.5.1 *Gamma-Ray Sensitivity*—Gamma-rays create a significant limitation for NRE measurements. Above a gamma-ray exposure of approximately 3R, NRE can become fogged by gamma-ray induced electron events. At this level of gamma-ray exposure, neutron induced proton-recoil tracks can no longer be accurately measured. As a consequence, NRE experiments are limited to low power environments such as found in critical assemblies and benchmark fields. Moreover, applications are only possible in environments where the buildup of radioactivity, for example, fission products, is limited.

1.5.2 *Low Energy Limit*—In the measurement of track length for proton recoil events, track length decreases as proton-recoil energy decreases. Proton-recoil track length below approximately 3μ in NRE can not be adequately measured with optical microscopy techniques. As proton-recoil track length decreases below approximately 3μ, it becomes very difficult to measure track length accurately. This 3μ track length limit corresponds to a low energy limit of applicability in the range of approximately 0.3 to 0.4 MeV for neutron induced proton-recoil measurements in NRE.

1.5.3 *Track Density Limit*—The ability to measure proton recoil track length with optical microscopy techniques depends on track density. Above a certain track density, a maze or labyrinth of tracks is created, which precludes the use of optical microscopy techniques. For manual scanning, this limitation arises above approximately 10^{4} tracks/cm^{2}, whereas interactive computer based scanning systems can extend this limit up to approximately 10^{5} tracks/cm^{2}.

1.6 *Neutron Spectrometry (Differential Measurements)*—For differential neutron spectrometry measurements in low

[1] This specification is under the jurisdiction of ASTM Committee E10 on Nuclear Technology and Applications, and is the direct responsibility of Subcommittee E10.05 on Nuclear Radiation Metrology.

Current edition approved June 10, 2000. Published August 2000.

[2] The boldface numbers in parentheses refer to the list of references at the end of the text.

power reactor environments, NRE experiments can be conducted in two different modes. In the more general mode, NRE are irradiated in-situ in the low power reactor environment. This mode of NRE experiments is called the 4π mode, since the in-situ irradiation creates tracks in all directions (see 3.1.1). In special circumstances, where the direction of the neutron flux is known, NRE are oriented parallel to the direction of the neutron flux. In this orientation, one edge of the NRE faces the incident neutron flux, so that this measurement mode is called the end-on mode. Scanning of proton-recoil tracks is different for these two different modes. Subsequent data analysis is also different for these two modes (see 3.1.1 and 3.1.2).

1.7 *Neutron Dosimetry (Integral Measurements)*—NRE also afford integral neutron dosimetry through use of the (n,p) reaction in low power reactor environments. Two different types of (n,p) integral mode dosimetry reactions are possible, namely the I-integral and the J-integral **(10,11)**. Proton-recoil track scanning for these integral reactions is conducted in a different mode than scanning for differential neutron spectrometry (see 3.2). Integral mode data analysis is also different than the analysis required for differential neutron spectrometry (see 3.2). This practice will emphasize NRE (n,p) integral neutron dosimetry, because of the utility and advantages of integral mode measurements in low power benchmark fields.

2. Referenced Documents

2.1 *ASTM Standards:*

E 706 Matrix for Light Water Reactor Pressure Vessel Surveillance Standards[3]

E 854 Test Method for Application and Analysis of Solid State Track Recorders (SSTR) Monitors for Reactor Surveillance[3]

E 910 Test Method for Application and Analysis of Helium Accumulation Fluence Monitors (HAFM) for Reactor Vessel Surveillance[4]

E 944 Guide for Application of Neutron Spectrum Adjustment Methods in Reactor Surveillance[3]

E 1005 Test Method for Application and Analysis of Radiometric Monitors for Reactor Vessel Surveillance[3]

3. Alternate Modes of NRE Neutron Measurements

3.1 *Neutron Spectrum Measurements*—The neutron energy range of interest in reactors environments covers approximately nine orders of magnitude, extending from thermal energies up to approximately 20 MeV. No single method of neutron spectrometry exists that can completely cover this energy range of interest **(12)**. Work with proton-recoil proportional counters has not been extended beyond a few MeV, due to the escape of more energetic protons from the finite sensitive volume of the counter. In fact, correction of in-situ proportional counters for such finite-size effects can be non-negligible above 0.5 MeV **(13)**. Finite-size effects are much more manageable in NRE because of the reduced range of recoil protons. As a consequence, NRE fast neutron spectrometry has been applied at energies up to 15 MeV **(3)**. For in-situ spectrometry in reactor environments, NRE measurements up to 8.0 MeV are possible with very small finite-size corrections **(14-16)**.

3.1.1 *4π Mode*—It has been shown **(3-6)** that a neutron fluence-spectrum can be deduced from the integral relationship

$$M(E) = n_p\, V \int_E^{\infty} \frac{\sigma_{np}(E)\, \Phi(E)}{E}\, dE \qquad (1)$$

where:

$\Phi(E)$ = neutron fluence in n/(cm^2–MeV),
$\sigma_{np}(E)$ = neutron-proton scattering cross section (cm^2) at neutron energy, E,
E = neutron or proton energy (MeV),
n_p = atomic hydrogen density in the NRE (atoms/cm^3),
V = volume of NRE scanned (cm^3), and
$M(E)$ = proton spectrum (protons/MeV) observed in the NRE volume V at energy E.

The neutron fluence can be derived from Eq 1 and takes the form:

$$\Phi(E) = \frac{-E}{\sigma_{np}(E) n_p V} \frac{dM}{dE} \qquad (2)$$

Eq 2 reveals that the neutron fluence spectrum at energy E depends upon the slope of the proton spectrum at energy E. As a consequence, approximately 10^4 tracks must be measured to give statistical accuracies of the order of 10 % in the neutron fluence spectrum (with a corresponding energy resolution of the order of 10 %). It must be emphasized that spectral measurements determined with NRE in the 4π mode are absolute.

3.1.2 *End-On Mode*—Differential neutron spectrometry with NRE is considerably simplified when the direction of neutron incidence is known, such as for irradiations in collimated or unidirectional neutron beams. In such exposures, the kinematics of (n,p) scattering can be used to determine neutron energy. Observation of proton-recoil direction and proton-recoil track length provide the angle of proton scattering relative to the incident neutron direction θ and the proton energy E_p, respectively. In terms of these observations, the neutron energy E_n is simply:

$$E_n = \frac{E_p}{\cos^2 \theta} \qquad (3)$$

In collimated or unidirectional neutron irradiations, the emulsion is exposed end-on as depicted in Fig. 1. The end-on mode can be used to advantage in media where neutron scattering is negligible for two types of benchmark field experiments, namely:

3.1.2.1 Benchmark field validation of the NRE method or characterization of point neutron sources, for example, the standard ^{252}Cf neutron field at the National Institute of Standards and Technology (NIST) **(17)**.

3.1.2.2 Measurement of leakage neutron spectra at sufficiently large distances from the neutron source, for example, neutron spectrum measurements at the Little Boy Replica (LBR) benchmark field **(18)**.

3.2 *Integral Mode*—It is possible to use emulsion data to obtain both differential and integral spectral information. Emulsion work is customarily carried out in the differential

[3] *Annual Book of ASTM Standards*, Vol 02.02.
[4] *Annual Book of ASTM Standards*, Vol 14.02.

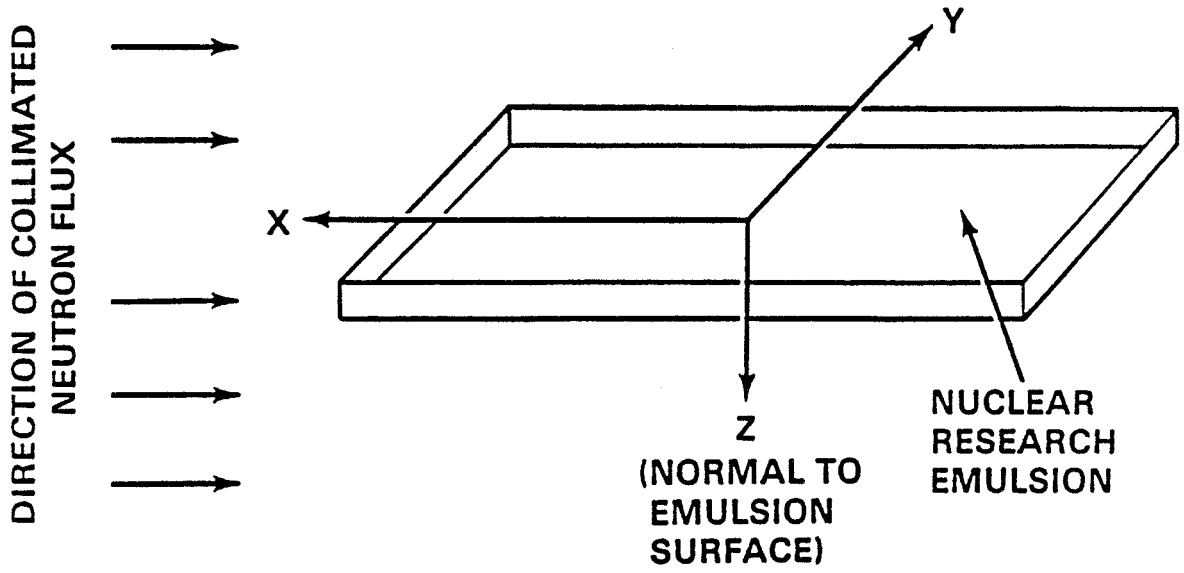

FIG. 1 Geometrical Configuration for End-On Irradiation of NRE

mode **(3-6)**. In contrast, NRE work in the integral mode is a more recent concept and, therefore, a fuller explanation of this approach is included below. In this integral mode, NRE provide absolute integral reaction rates, which can be used in spectral adjustment codes. Before these recent efforts, such codes have not utilized integral reaction rates based on NRE. The significance of NRE integral reaction rates stems from the underlying response, which is based on the elastic scattering cross section of hydrogen. This σ_{np} (E) cross section is universally accepted as a standard cross section and is known to an accuracy of approximately 1 %.

3.2.1 *The I Integral Relation*—The first integral relationship follows directly from Eq 1. The integral in Eq 1 can be defined as:

$$I(E_T) = \int_{E_T}^{\infty} \frac{\sigma\,(E)}{E}\,\Phi(E)\,dE \tag{4}$$

Here $I\,(E_T)$ possesses units of proton-recoil tracks/MeV per hydrogen atom. Clearly $I\,(E_T)$ is a function of the lower proton energy cut-off used for analyzing the emulsion data. Using Eq 4 in Eq 1, one finds the integral relation:

$$I(E_T) = \frac{M(E_T)}{n_p V} \tag{5}$$

$I\,(E_T)$ is evaluated by using a least squares fit of the scanning data in the neighborhood of $E = E_T$. Alternatively, since:

$$M(E_T) = M(R_T)\,\frac{dR(E)}{dE} \tag{6}$$

where: $R\,(E)$ is the proton-recoil range at energy E in the NRE and dR/dE is known from the proton range-energy relation for the NRE. One need only determine $M\,(R)$ in the neighborhood of $R = R_T$. Here M(R) is the number of proton-recoil tracks/micron observed in the NRE. Consequently, scanning efforts can be concentrated in the neighborhood of $R = R_T$ in order to determine $I\,(E_T)$. In this manner, the accuracy attained in $I\,(E_T)$ is comparable to the accuracy of the differential determination of $\Phi(E)$, as based on Eq 2, but with a significantly reduced scanning effort.

3.2.2 *The J Integral Relation*—The second integral relation can be obtained by integration of the observed proton spectrum $M\,(E_T)$. From Eq 1:

$$\int_{E_{\min}}^{\infty} M(E_T)dE_T = n_p V \int_{E_{\min}}^{\infty} dE_T \int_{E_T}^{\infty} \frac{\sigma(E)}{E}\,\Phi(E)dE \tag{7}$$

where: $E_{\min}$ is the lower proton energy cut-off used in analyzing the NRE data. Introducing into Eq 7 the definitions:

$$\mu(E_{\min}) = \int_{E_{\min}}^{\infty} M(E_T)dE_T \tag{8}$$

and:

$$J(E_{\min}) = \int_{E_{\min}}^{\infty} dE_T \int_{E_T}^{\infty} \frac{\sigma(E)}{E}\,\Phi(E) \tag{9}$$

has:

$$J(E_{\min}) = \frac{\mu(E_{\min})}{n_p V} \tag{10}$$

Hence, the second integral relation, namely Eq 10, can be expressed in a form analogous to the first integral relation, namely Eq 5. Here $\mu(E_{\min})$ is the integral number of proton-recoil tracks per hydrogen atom observed above an energy $E_{\min}$ in the NRE. Consequently the integral $J\,(E_{\min})$ possesses units of proton-recoil tracks per hydrogen atom. The integral $J\,(E_{\min})$ can be reduced to the form:

$$J(E_{\min}) = \int_{E_{\min}}^{\infty} \left(1 - \frac{E_{\min}}{E}\right)\sigma(E)\Phi(E)dE \tag{11}$$

In addition by using Eq 6, the observable $\mu(E_{\min})$ can be expressed in the form:

$$\mu(E_{\min}) = \int_{R_{\min}}^{\infty} M(R)dR \tag{12}$$

Hence, to determine the second integral relationship, one need only count proton-recoil tracks above $R = R_{\min}$. Tracks considerably longer than $R_{\min}$ need not be measured, but simply counted. However, for tracks in the neighborhood of $R = R_{\min}$, track length must be measured so that an accurate lower bound $R_{\min}$ can be effectively determined.

4. Significance and Use

4.1 *Integral Mode Dosimetry*—As shown in 3.2, two different integral relationships can be established using proton-recoil emulsion data. These two integral reactions can be obtained with roughly an order of magnitude reduction in scanning effort. Consequently this integral mode is an important complementary alternative to the customary differential mode of NRE spectrometry. The integral mode can be applied over extended spatial regions, for example, perhaps up to as many as ten in-situ locations can be covered for the same scanning effort that is expended for a single differential measurement. Hence the integral mode is especially advantageous for dosimetry applications which require extensive spatial mapping, such as exist in Light Water Reactor-Pressure Vessel (LWR-PV) benchmark fields (see Test Method E 1005). In low power benchmark fields, NRE can be used as integral dosimeters in a manner similar to RM, solid state track recorders (SSTR) and helium accumulation monitors (HAFM) neutron dosimeters (see Test Methods E 854 and E 910). In addition to spatial mapping advantages of these other dosimetry methods, NRE offer fine spatial resolution and can therefore be used in-situ for fine structure measurements. In integral mode scanning, both absolute reaction rates, that is $I(E_T)$ and $J(E_{min})$, are determined simultaneously. Separate software codes need to be used to permit operation of a computer based interactive system in the integral mode (see Section 9). It should be noted that the integrals $I(E_T)$ and $J(E_{min})$ possess different units, namely proton-recoil tracks/MeV per hydrogen atom and proton-recoil tracks per hydrogen atom, respectively.

4.2 *Applicability for Spectral Adjustment Codes*—In the integral mode, NRE provide absolute integral reaction rates that can be used in neutron spectrum least squares adjustment codes (see Guide E 944). In the past, such adjustment codes could not utilize NRE integral reaction rates because of the non-existence of NRE data. NRE integral reaction rates provide unique benchmark data for use in least squares spectral adjustment codes. The unique significance of NRE integral data arises from a number of attributes, which are described separately below. Thus, inclusion of NRE integral reaction rate data in the spectral adjustment calculations can result in a significant improvement in the determination of neutron spectra in low power benchmark fields.

4.3 *The Neutron Scattering Cross Section of Hydrogen*—Integral NRE reaction rates are based on the standard neutron scattering cross section of hydrogen. For fast neutron spectrometry and dosimetry applications, the accuracy of this (n,p) cross section over extended energy regions is essentially unmatched. A semi-empirical representation of the energy-dependence of the (n,p) cross section is given in Eq 13.

$$\sigma_{np}(E) = 3\pi\,[1.206E + (-1.860 + 0.0941491E + 0.000130658E^2)^2]^{-1} + \pi[1.206E + (0.4223 + 0.1300E)^2]^{-1} \quad (13)$$

where: E is in MeV and $\sigma_{np}(E)$ is in barns. This energy-dependent representation of the (n,p) cross section possesses an uncertainty of approximately 1 % at the (1σ) level **(19)**.

4.4 *Threshold Energy Definition*—In contrast with all other fast neutron dosimetry cross sections, the threshold energy of the I and J integral reaction rates can be varied. NRE integral reaction threshold variability extends down to approximately 0.3 to 0.4 MeV, which is the lower limit of applicability of the NRE method. Threshold variation is readily accomplished by using different lower bounds of proton track length to analyze NRE proton-recoil track length distributions. Furthermore, these NRE thresholds are more accurately defined than the corresponding thresholds of all other fast neutron dosimetry cross sections. NRE therefore provide a response with an extremely sharp energy cutoff that is not only unmatched by other cross sections, but an energy threshold that is independent of the in-situ neutron spectrum. No other fast neutron dosimetry cross sections possess a threshold response with these significant attributes. The behavior of the I-integral and J-integral response for different threshold energies is shown in Figs. 2 and 3, respectively, in comparison to the threshold $^{237}Np(n,f)$ reaction used in RM dosimetry.

4.5 *Complimentary Energy Response*—It is of interest to compare the differential energy responses available from these two integral relations. From Eq 4 and 11, one finds responses of the form $\sigma(E)/E$ and $(1 - E_{min}/E)\sigma(E)$ for the I and J integral relations, respectively. These two responses are compared in Fig. 4 using a common cut-off of 0.5 MeV for both E_T and E_{min}. Since these two responses are substantially different, simultaneous application of these two integral relations would be highly advantageous. As shown in Fig. 4, the energy response of the I and J integral reaction rates compliment each other. The J-integral response increases with increasing neutron energy above the threshold value and therefore possesses an energy dependence qualitatively similar to most fast neutron dosimetry cross sections. However, significant quantitative differences exist. As discussed above, the J-integral response is more accurately defined in terms of both the energy-dependent cross section and threshold energy definition. The I-integral possesses a maximum value at the threshold energy and decreases rapidly from this maximum value as neutron energy increases above the threshold value. As can be seen in Fig. 4, the I-integral possesses a much more narrowly defined energy response than the J-integral. While the J-integral response is

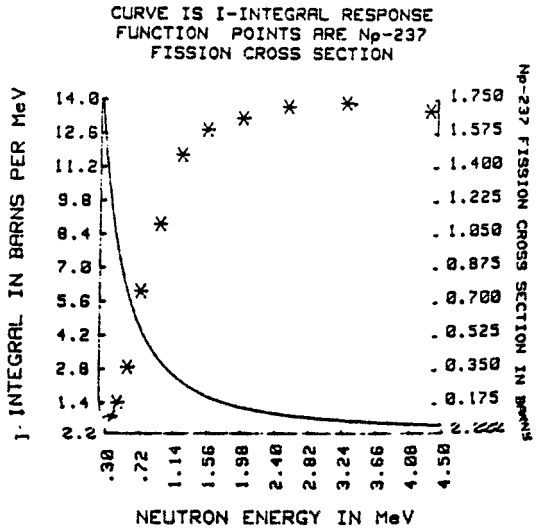

FIG. 2 Comparison of the I-Integral Response with the ^{237}Np (*n,f*) Threshold Reaction

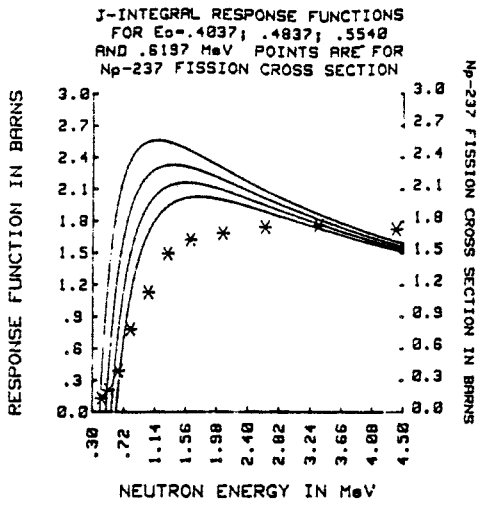

FIG. 3 Comparison of the J-Integral Response for E_T = 0.404, 0.484, 0.554 and 0.620 MeV with the ^{237}Np (*n,f*) Threshold Reaction

broadly distributed, most of the I-integral response is concentrated in the neutron energy just above threshold. As a consequence, the I-integral reaction rate data generally provides a more rigorous test of the ability of neutron transport calculations to describe the complex spatial and energy variations that exist in benchmark fields than does the J-integral data. This conclusion is supported by the calculation to experiment ratios (C/E) obtained from NRE experiments in the VENUS-1 LWR-PV benchmark field. For these VENUS-1 NRE experiments, the C/E values for the I integral possessed larger variation and deviated more widely from unity than the corresponding C/E values for the J-integral **(20)**.

5. Apparatus

5.1 *Dark Room*—A dark room equipped with a sink, processing baths and a safe light. There should be adequate bench space in the dark room for pre-irradiation preparation of NRE as well as for the transfer of NRE between processing trays.

5.2 *Constant Temperature Baths*—The constant temperature baths in the dark room should posses temperature control to 0.1°C. One cooling bath should be equipped with a circulating pump so that tap water can be circulated through the coils of the processing bath. One thermostatically controlled processing bath.

5.3 *Refrigerator*—The dark room should be equipped with a refrigerator for storing reagents and chemicals.

5.4 *Stainless Steel Trays*—Stainless steel (SS) trays and cover lids are required, approximately 25 by 15 cm in area by 2.5 cm deep, for NRE processing.

5.5 *Racks*—Racks are required to position and hold the SS trays in the constant temperature baths. These racks hold the SS trays in the constant temperature bath so that the top of the SS trays project above the bath surface by approximately 0.5 cm.

5.6 *Cooling Coil*—A cooling coil is required that is immersed in the constant temperature bath which and connected by a suitable tube to the cold water tap. Another identical tube must serve as a drain line from the cooling coil to the sink. An in-line valve for control of tap water flow should be installed so that a small steady stream of water can be regulated.

5.7 *Optical Microscopes*—Optical microscopes are required for NRE scanning with a magnification of 1000X or higher, utilizing oil immersion techniques. Microscope stages should be graduated with position readout to better than 1 µm and should also possess at least 1 µm repositioning accuracy. The depth of focus (z-coordinate) should be controlled to the nearest 0.1 µm with similar repositioning accuracy. Calibrated stage micrometers and graduated eyepiece grids (reticles) are also required for track scanning.

5.8 *Filar Micrometer*—A filar micrometer is required for measuring thickness with electronic readout to at least the nearest 0.1 µm.

5.9 *Dial Gages*—Dial thickness gages are required with readout scales of at least 2 µm per division.

5.10 *Scribes*—Diamond point scribes are required for marking NRE glass backing with suitable pre-irradiation identification labels

5.11 *Thermometers*—Thermometers are required for measuring temperature with readout to at least the nearest 0.1°C.

5.12 *Interactive Scanning System*—A computer based interactive scanning system is required for the measurement of proton-recoil track length in NRE. Hardware and software requirements are described in Section 9.

6. Reagents and Materials

6.1 *Purity of Reagents*—Distilled or demineralized water and analytical grade reagents should be used at all times.

6.2 *Reagents*—Tables 1-4 provide detailed specifications for the processing solutions.

6.2.1 *Developing Solution*—As specified in Table 1, Amidol, 2,4–Diaminophenol Dihydrochloride is used to develop the NRE (Eastman Organic Chemicals, No. P 614, other commercially prepared amidol developers also work well.) The anti-fog solution specified in Table 2 is used to suppress chemical fog and prevent the development of gamma-ray induced electron tracks and thereby improve proton-recoil track length measurements.

6.2.2 *Stop Bath Solution*—The stop bath solution should be a 1 % glacial acedic acid in distilled water.

6.2.3 *Fixing Solution*—A fixing solution containing sodium thiosulfate (hypo) and sodium bisulfite is required (see Table 3).

6.2.4 *Drying Solutions*—Two drying solutions of glycerine, ethyl alcohol, and distilled water are required (see Table 4).

6.3 *Materials*:

6.3.1 *Emulsions*—Ilford type L-4 NRE, 200 and 400 µm thick pellicles, mounted on glass backing. The glass backing is approximately 2.5 by 7.5 cm in area by 1 mm thick.

7. Pre-Irradiation NRE Preparation

7.1 *NRE Preparation*—The NRE should be cut to an acceptable size in the dark room. A safe light with a yellow filter may be used. The diamond point scribe should be used to rule the glass backing undersurface of the NRE and the glass backing can then be snapped along the rule marks to obtain the desired NRE dosimeter size. NRE dosimeters down to approximately 5 by 5 mm area can be readily obtained. The diamond point scribe should then be used to mark an ID number on the undersurface of the glass backing. The NRE should then be

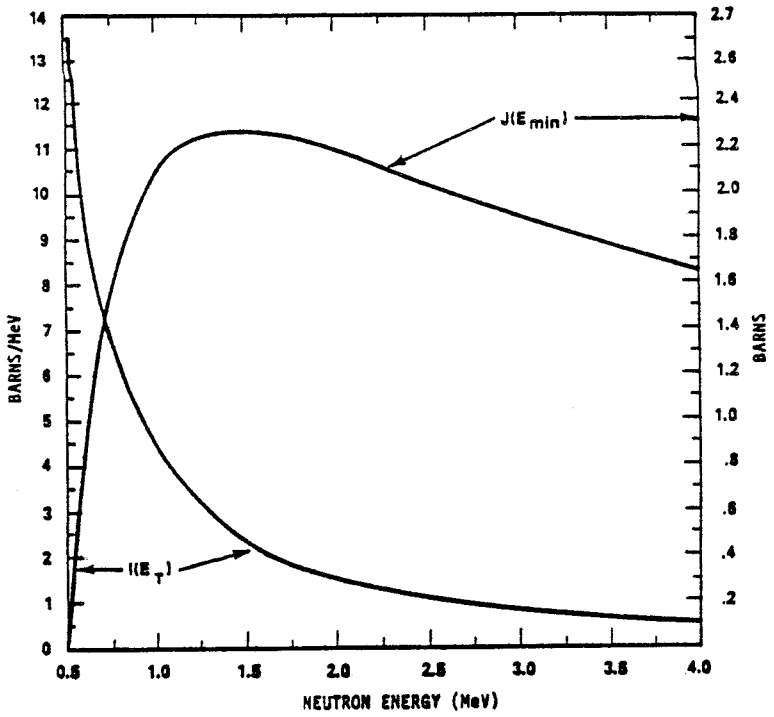

FIG. 4 Energy Dependent Response for the Integral Reactions $I(E_T)$ and $J(E_{min})$

TABLE 1 Developing Solution[A]

Reagent	Volume/Mass
Distilled Water	1.0 L
Boric Acid Crystals	3.0 g
Potassium Bromide	1.0 g
Desiccated Na_2SO_3	50 g
Amidol	2.0 g
Anti-Fog Solution	6.0 cc

[A]Chemicals dissolved in order listed at room temperature.

TABLE 2 Anti-Fog Stock Solution

Reagent	Volume/Mass
Ethylene Glycol (50°C)	175 cc
Kodak Anti-Fog #1[A]	41.68 g
Ethylene Glycol	≈ 75 cc[B]

[A]Dissolve in warm ((50°C)) Ethylene Glycol
[B]Cool to 24°C and Add cool Ethylene glycol to make 250 cc.

TABLE 3 Fixing Solution[A]

Reagent	Volume/Mass
Distilled Water	1 L
$Na_2S_2O_3$(Hypo)	400 g
$NaHSO_3$[B]	10 g

[A]Chemicals dissolved in order listed at room temperature.
[B]If $Na_2S_2O_5$ is used, decrease mass by a factor of 0.87.

TABLE 4 Drying Solutions

	Volume, %	
Reagent	Solution 1	Solution 2
Distilled Water	35	0.00
Glycerine	30	30
Ethyl Alcohol (95%)[A]	35	70

[A]Absolute alcohol should not be used, since it contains traces of benzene.

wrapped in lens paper and then in aluminum foil (~0.002 cm thick) for further handling and to prevent exposure to light. The NRE ID number can then be written on the Al-foil wrapping with an indelible pen. If it is necessary to know the orientation of the NRE in the irradiation field, the undersurface NRE glass backing is marked with an indelible pen to provide a known orientation for the NRE. This marking orientation must then be transcribed to the Al-foil wrapping. The NRE can then be removed from the dark room. However, if the NRE are to be deployed in Al or Cd buckets for the irradiation, this assembly procedure should also be conducted in the dark room if at all possible. It will then be necessary to transcribe the NRE ID number and orientation information to the outer surface of the irradiation bucket. A knowledge of NRE orientation together with a complete record of proton-recoil scanning data (see Section 9 can then be used to determine any anisotropy of the in-situ neutron field.

7.2 *NRE Thickness Measurement*—To measure the original thickness of the emulsion, HO, place the glass undersurface of the NRE on a flat surface in the dark room. Use the dial thickness gauge to measure the thickness of the emulsion and glass backing. Repeat this measurement five to ten times so that a precise average is obtained. The glass backing thickness is determined after irradiation and post-irradiation processing (see 8.8).

8. Post-Irradiation Processing Procedures

8.1 Processing procedures will depend to some extent on the particular batch of Ilford NRE that are used. Consequently, while the processing procedures recommended below will not necessarily be optimum for any given batch, these procedures can be used as a starting point to attain optimum procedures desired for the specific NRE neutron dosimetry application under consideration. Table 5 summarizes the various steps utilized in the post-irradiation NRE processing procedures.

TABLE 5 Summary of NRE Processing Steps

Step	Solution	Temperature, °C	Time Duration	
			200μ[A]	400μ[A]
Pre-soaking	Distilled H_2O	2	1h	2h
Developing-1	See Tables 1 and 2	1.2	1h	2.5h
Developing-2	See Tables 1 and 2	5	35 to 40 min	35 to 40 min
Stop Bath	1 % Glacial Acedic Acid	5	15 to 20 min	1h
Fixing	See Table 3	5	2h to 1 Day	2 to 3 Days
Washing	Tap Water	6	1 Day	1 Day
Drying-1	See Table 4	5	1h	2.5 h
Drying-2	See Table 4	5	1h	2.5 h

[A]Ilford L-4 NRE thickness in microns.

8.1.1 *Pre-Soaking Step*—Use a mixture of approximately 50 % distilled water and 50 % ethylene glycol in the cooling bath to maintain a temperature of 2°C. Fill a SS tray with distilled water. Pre-cool the distilled water soaking solution to 5°C before inserting the NRE into the distilled water. This will keep the NRE swelling to a minimum. Insert the SS trays into the 2°C bath. The purpose of the pre-soaking step is to facilitate uniform penetration of the Amidol developer throughout the full thickness of the NRE. In this way, development will be uniform, that is, independent of depth (denoted by the z coordinate). Pre-soak 200μ L-4 NRE for 1 h and 400μ L-4 NRE for 2 h.

8.2 *Developing Step at 1.2°C*—Prepare a fresh development solution as prescribed in Tables 1 and 2. Place the development solution in a SS tray and insert the tray into the cooling bath at 1.2°C. Transfer the NRE directly from the pre-soaking solution to the development solution. The rate of NRE development is very sensitive to the temperature of the developer. Use of the low 1.2°C temperature provides enhanced developer penetration with very little actual development. The length of time the NRE remain in the 1.2°C developer depends on the NRE thickness. Develop Ilford L-4 200 and 400μ NRE for approximately 1 h and 2.5 h, respectively.

8.3 *Developing Step at 5°C*—Transfer the tray containing the NRE in the development solution from the cooling bath at 1.2°C to the processing bath which is maintained at 5°C. Here a development time of approximately 35 to 40 min can be used, independent of NRE thickness.

8.4 *Stop-Bath Step*—The stop-bath solution (1 % glacial acedic acid in distilled water) should be pre-mixed and stored in a plastic bottle in the refrigerator. Fill another SS tray with stop-bath solution and place the tray in the processing tank so it cools to the 5°C temperature of the processing bath. Remove both trays from the processing bath and place the trays on a convenient flat surface in the dark room. Rapidly transfer the NRE from the developer tray into the stop-bath tray and place the stop-bath tray back into the processing bath. Care should be exercised to avoid touching the NRE surface. The NRE should be handled by holding the glass backing. The time duration that the NRE remain in the stop-bath solution depends on NRE thickness. For 200 μm NRE, approximately 15 to 20 min will do, whereas approximately 60 min should be used for 400 μm NRE. The stop-bath solution changes the ph of the NRE to stop development.

8.5 *Fixing Solution Step at 5°C*—The fixing solution (see Table 3) should be pre-mixed and stored in a plastic bottle in the refrigerator. Remove the fixing solution from the refrigerator and fill a SS tray at least half-way with the fixing solution. Place the SS tray in the processing bath until the fixing solution comes to equilibrium at 5°C. Remove both the stop-bath tray and the fixing solution trays from the processing bath onto a convenient flat surface in the dark room. Rapidly transfer the NRE from the stop-bath tray to the fixing solution tray. Replace the fixing solution tray back into the processing bath. The fixing solution dissolves the undeveloped silver bromide grains in the NRE, so that the NRE become transparent for track scanning purposes. The residence time of the NRE in the fixing solution depends on NRE thickness. For 200 μm NRE, it takes several hours to a day. For 400 μm NRE, it can take several days. The NRE should remain in the fixing solution approximately 1.5 times the time duration that it takes for the NRE to clear. When using the fixing solution for several days, as needed for the 400 μm NRE, replenish the fixing solution at least once a day by pouring off 50 % of the old solution and adding 50 % new fixing solution.

8.6 *NRE Washing*—The fixing solution needs to be thoroughly removed from the NRE. This washing process can be done in daylight. Actually, the darkroom (bright) lights can be turned on as soon as the fixing process is completed. Wash the NRE with a stream of tap water, which runs through coils at the bottom of the 1.2°C cooling bath. Let cold tap water run slowly through a tube to the coils in the cooling bath and then through a tube to an empty SS tray in the sink. A good control valve is needed on the tube carrying the cold tap water so as to ensure a good even flow of water. When the water in the tray has reaches a temperature of ≈6°C, transfer the fixed emulsions from the SS tray in the 5°C bath to the tray in the sink. The tap water should run into the SS tray slowly so as not to produce a significant stream that might distort the emulsions. The NRE should be washed in this manner for approximately 24 h.

8.7 *Drying Solution Steps*—The NRE obtained from the washing step are swelled with water to two to three times the original thickness. The purpose of the drying solution step is to remove the water and thereby reduce distortion and at the same time provide for more precise thickness (z-coordinate) measurements. Two drying solutions are prepared as prescribed in Table 4. The two drying solutions are placed into SS trays and allowed to come to equilibrium in the 5°C processing bath. Using some convenient flat surface in the dark room, the NRE are transferred from the washing tray to SS tray containing the first drying solution. The SS tray containing the NRE in the first drying solution is placed in the 5°C processing tank for approximately 1 h for 200μ NRE and 2.5 h for 400μ NRE. This step is repeated with the second drying solution. Upon removal from the second drying solution, the NRE can be placed (emulsion side up) on a flat surface so that the NRE can be gently blotted to remove the excess drying solution. The NRE are then air dried at room temperature for at least 24 h. In this drying process, the water in the NRE is replaced with alcohol which, in turn, evaporates and glycerine replaces the silver bromide that was in the unprocessed emulsions. (Actually, the glycerine fills the holes from which the silver bromide was removed in the fixing process.)

8.8 *Post-Irradiation NRE Thickness Measurements*—After

processing is complete, place the NRE on edge under a microscope equipped with a filar micrometer eyepiece. Measure the glass backing and processed emulsion thickness separately. Make 5 to 10 observations of each thickness so that a precise average of both the emulsion thickness and the glass backing thickness can be determined. These data provide the processed NRE thickness, HP, and the glass backing thickness can then be used with the pre-irradiation thickness measurements to determine the original NRE thickness, HO. To obtain the true z-coordinate position in the (irradiated) NRE, z_{tr}, from the observed z-coordinate, z_{obs}, one must use the relation

$$z_{tr} = \frac{HO}{HP} z_{obs} \tag{14}$$

8.9 *NRE Microscope Mounting*—The processed NRE is mounted on a watch glass (microscope cover glass), which is cemented in a rigid frame that can, in turn, be attached to the microscope stage. When NRE are not being scanned, they should be stored in Petrie dishes under controlled temperature and humidity conditions. Standard room temperature is acceptable, but 50 % relative humidity is preferable, since the glycerine is somewhat hydroscopic. Large changes in humidity during storage should be avoided.

9. Track Scanning

9.1 *Instrumentation*—The principal disadvantage of the NRE method of fast neutron dosimetry is the need to measure proton-recoil track length for many tracks. Accurate differential spectrometry measurements require measurement of approximately 10^4 tracks, so that many hours of scanning are required. To facilitate proton-recoil track length measurements and provide a much more cost-effective measurement system, a computer-based interactive system is indispensable. Such a system can store all the (3D) scanning information, in detail, as well as provide on-line computations for individual track analysis. To conduct all of these operations manually would be impractical. Such a computer-based interactive system was built and used successfully for NRE neutron dosimetry some time ago **(17)**. The specifications and scanning procedures given here are based on this system, which was called the Emulsion Scanning Processor (ESP). Since the ESP system was built some time ago, many of the components of the ESP system are outdated because of the rapid development of computer technology that has ensued. Consequently, to fabricate such a system today, one should only use this description as an overall guide and replace all components with state-of-the-art components, which will be invariably faster, more reliable and less expensive.

9.1.1 *Overall Design*—Some of the major considerations in the development of an interactive system for NRE scanning are simplicity, ease of operation, stability, and reliability of performance. In the design of the interactive system, the flexibility and power of computer control should be utilized to the maximum possible extent. A photograph of the ESP system is provided in Fig. 5. Shown on the laboratory bench is the microscope, terminal, and joystick control boxes with push buttons. All other components are housed in the equipment rack. The major system components are listed in Table 6. Fig. 6 shows an overall interconnection block diagram of the ESP system. An operator must interact with the system to obtain the desired results. The joystick and push button controls are used to set parameters and boundaries, focus, locate tracks, measure track lengths, categorize, and store track data. The (*X, Y, Z*) stage motion, including depth, that is, focus, of the microscope is performed by the computer under operator control. The computer receives all operator instructions, moves the stage as directed, and stores positional information on command. Software programs, stored on computer disks, provide the flexibility needed to conveniently tailor operating, storage, and data presentation formats to satisfy different experiments and scanning modes.

9.2 *Scanning Coordinate Systems*—A Cartesian coordinate system (*G, R, S*) is used to describe field locations in the emulsion; whereas, another Cartesian coordinate system (*X, Y, Z*) is used to describe track-ending locations in the emulsion. The perimeters of a reticle located in the eyepiece of the microscope serve as the *G, R* boundaries of the field of view. The *S*-coordinate is the depth or focus coordinate. In using the interactive (ESP) system, the selected emulsion is divided into a number of field volumes. The volume of a field corresponds to the area of a field of view times the preselected depth of the emulsion as shown in Fig. 7. The distance ΔS is prescribed in order that scanning be primarily confined to the interior of the emulsion, where proton-recoil escape probabilities are either negligible or small. Hence, a field volume FV is given by the relation:

$$FV = \Delta G \cdot \Delta R \cdot S \tag{15}$$

To provide orientation for track scanning from day-to-day as well as between different scanners, a zero reference point must be chosen on the emulsion. To this end, a needle having a red dye on its tip is mounted on a microscope objective holder and is used to pierce the emulsion surface thereby leaving a red spot. A color microphotograph is taken of the spot. A proton track escaping from the top surface of the emulsion is selected near the spot. The zero reference point, *G* = O, *R* = O, *S* = O, is then stored as the point of escape of this proton-recoil track.

9.3 *Track Scanning*—The actual measurement of a typical track in an emulsion using the interactive ESP system is described below. Fig. 8 shows the ESP controls in more detail. Operations with the left (L) and right (R) push buttons are summarized in Table 7. The left joystick controls the *Z* (focus) position, whereas, the right joystick controls both *X* and *Y* positions. The design of the interactive system permits performance of all track scanning and recording activities without interrupting the observation of proton-recoil tracks in the NRE.

9.3.1 *Recording the Zero Reference Point*—The emulsion is clamped to the microscope stage, and a disk containing the operating program for the interactive (ESP) system is inserted in the computer system. The first step is to bring the zero reference point into focus under the reticle cross hair, that is, the exact center of the reticle grid. Pressing push button 3R (see Table 7) stores the coordinates of the zero reference point *G* = 0, *R* = 0, *S* = 0 on a (scanning) data disk.

9.3.2 *Field of View Parameters*—The scanner must then measure a number of parameters that are to be used in the analysis of the proton-recoil track scanning data. The field width ΔG and field height ΔR must both be measured. To

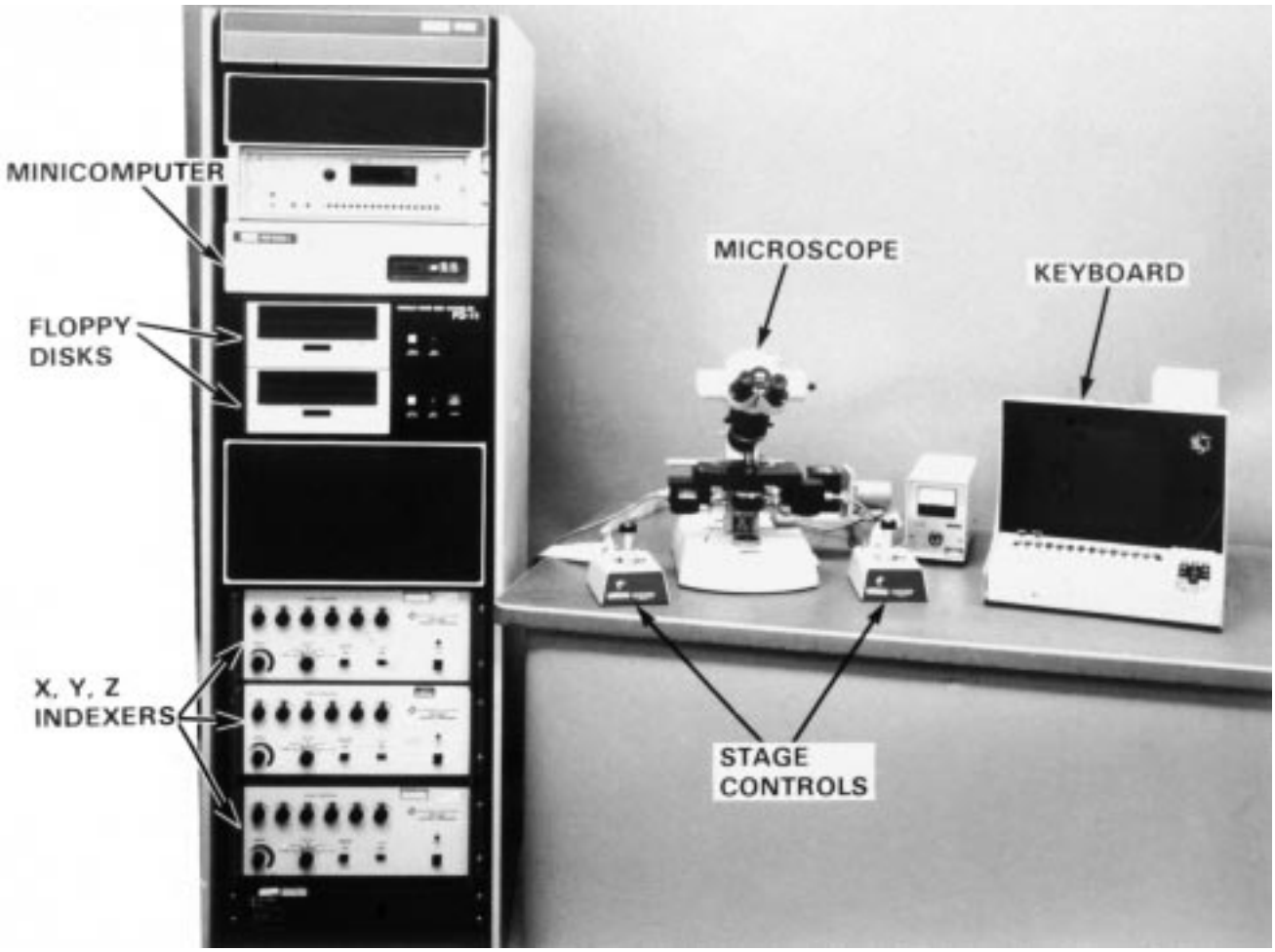

FIG. 5 Photograph of the Components Comprising the ESP System

TABLE 6 Equipment for the Emulsion Scanning Processor (ESP)

Component	Manufacturer
Universal Microscope System	Carl Zeiss
Computer Terminal	Beehive International
Joysticks	Tektronic
Computer	DEC PDP 11/03-L
Power Supply	DEC H740d
Dual Floppy Disk Drive	Charles River Data Systems
Indexers	Superior Electric SP153
Interface	J. F. Microsystem
Bus Expander	HEDL

measure the field width ΔG, a track ending is moved to the left edge of the field reticle and its position is stored. Next, the same track ending is moved to the right edge of the field reticle and its new position is stored, whereupon the computer will automatically retrace and calculate the field width ΔG in microns. The field height ΔR is measured in the same fashion except the track ending is moved to the top and bottom edges of the reticle. These measurements can be repeated to obtain average values for ΔG and ΔR in establishing field-of-view parameters. Other parameters that must be operator-prescribed include the area limits, G_{max} and R_{max}, which define the maximum traverses in the G and R directions, respectively, as shown in Fig. 9. In addition, the operator must enter the distance ΔS (which defines the interior emulsion depth S) as well as the original thickness, HO, of the NRE before processing. With these operations completed, the computer will calculate the number of fields of view contained within the boundary prescribed by G_{max} and R_{max} as depicted in Fig. 9.

9.3.3 *Field of View Selection*—The microscope is then automatically moved to a field of view to be scanned. Fields can be scanned either sequentially by rows, where consecutive fields are ordered according to the matrix (G_kR_j) or by directing the interactive system to a prescribed field (G_kR_j), which is obtained by entering the integers (k,j) at the computer keyboard.

9.3.4 *NRE Thickness Measurement*—When the field of view is reached, the emulsion thickness is measured by first focusing on the top surface, then on the bottom surface, and recording the respective S levels with push button 2R. The computer calculates the NRE thickness and automatically returns the focus to the preselected depth ΔS, as measured from the top of the emulsion (see Fig. 7). In this way, the thickness of the processed NRE is measured for each field that is scanned. The initials of the operator must be entered for each field scanned. This permits comparisons between scanning results of different individuals as well as comparisons between an individual scanner and the mean results obtained by a group of observers. Consequently, the objectivity and accuracy of any given

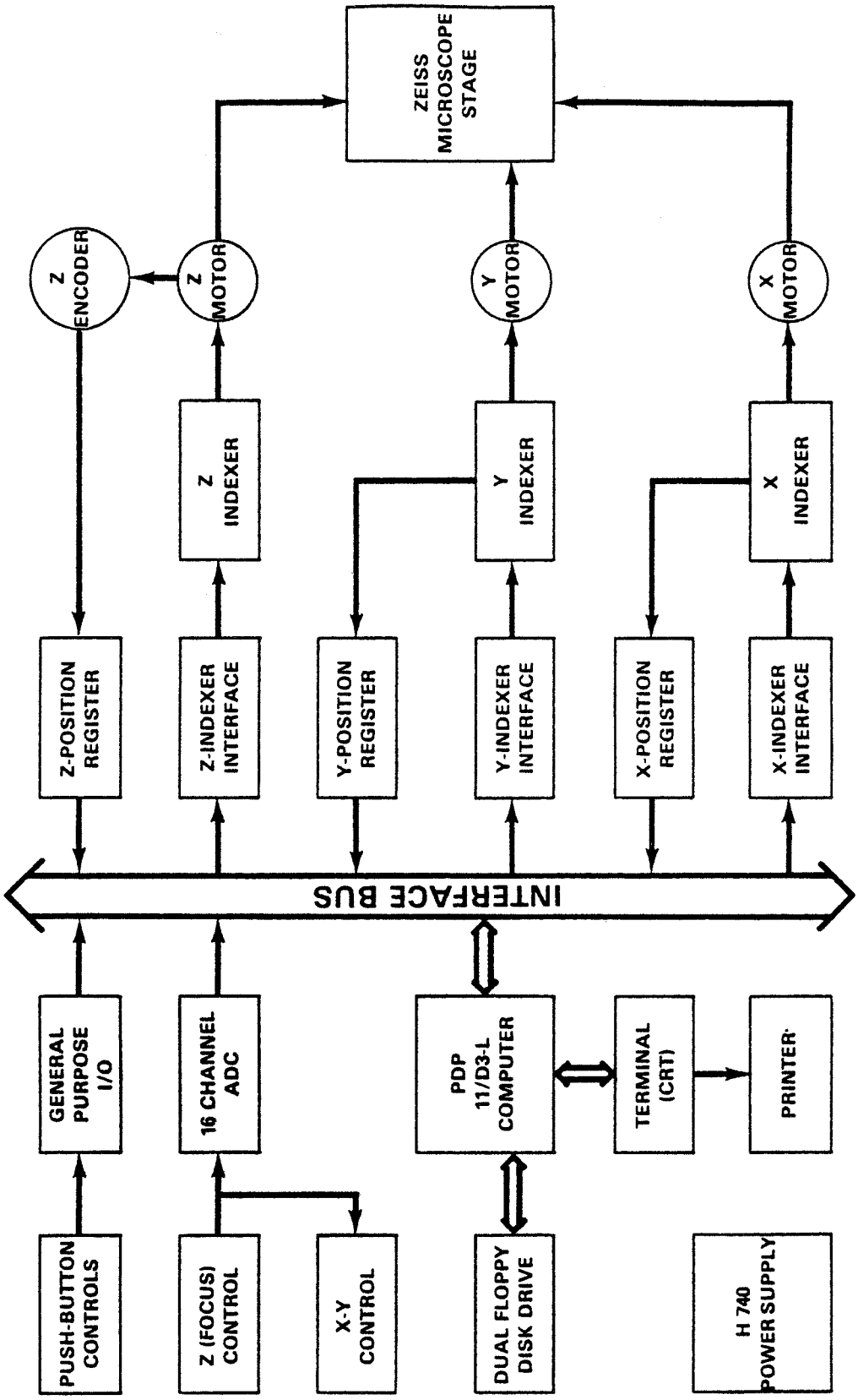

FIG. 6 Block Diagram of the ESP System

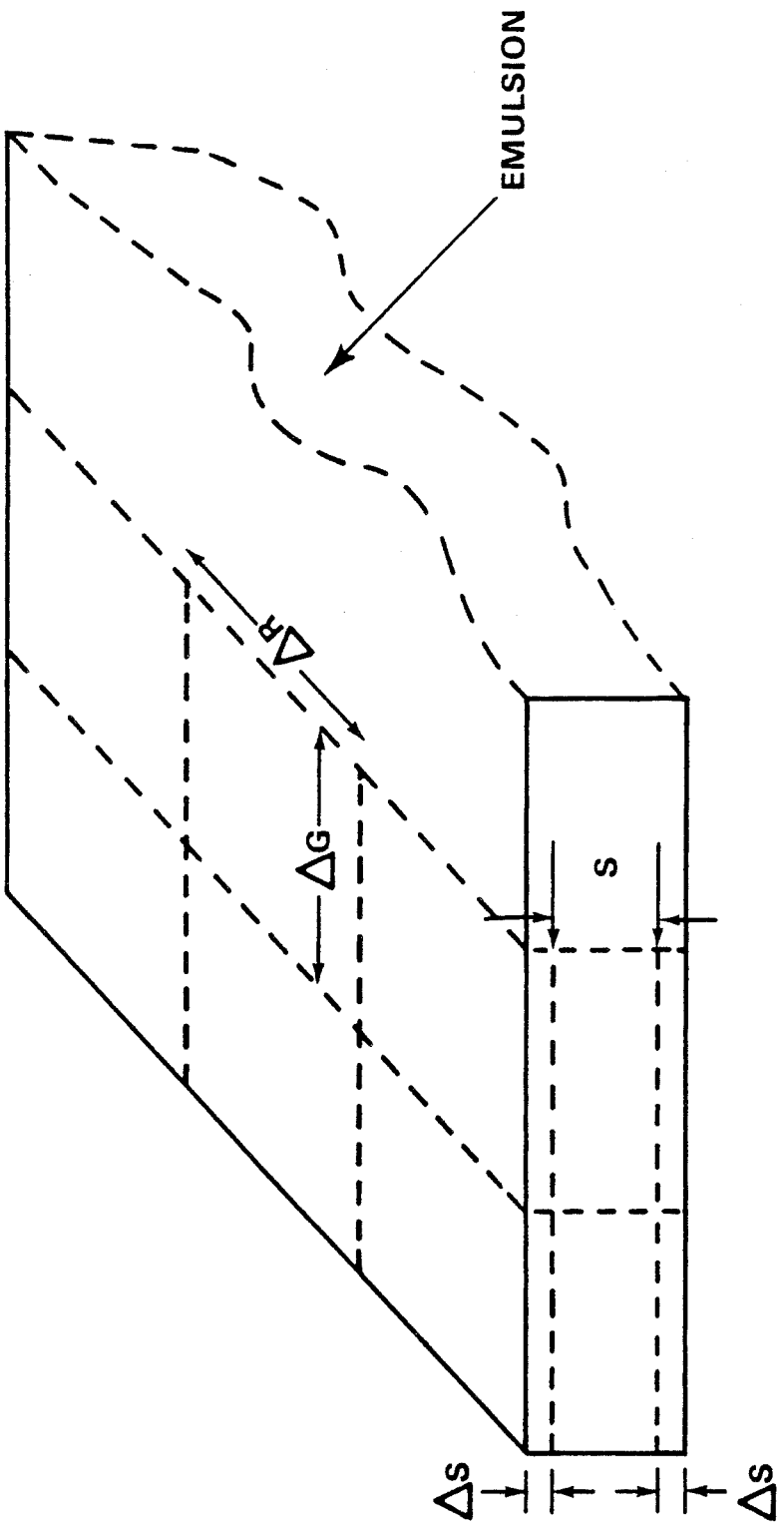

FIG. 7 Field Volume Coordinates Used for NRE Scanning

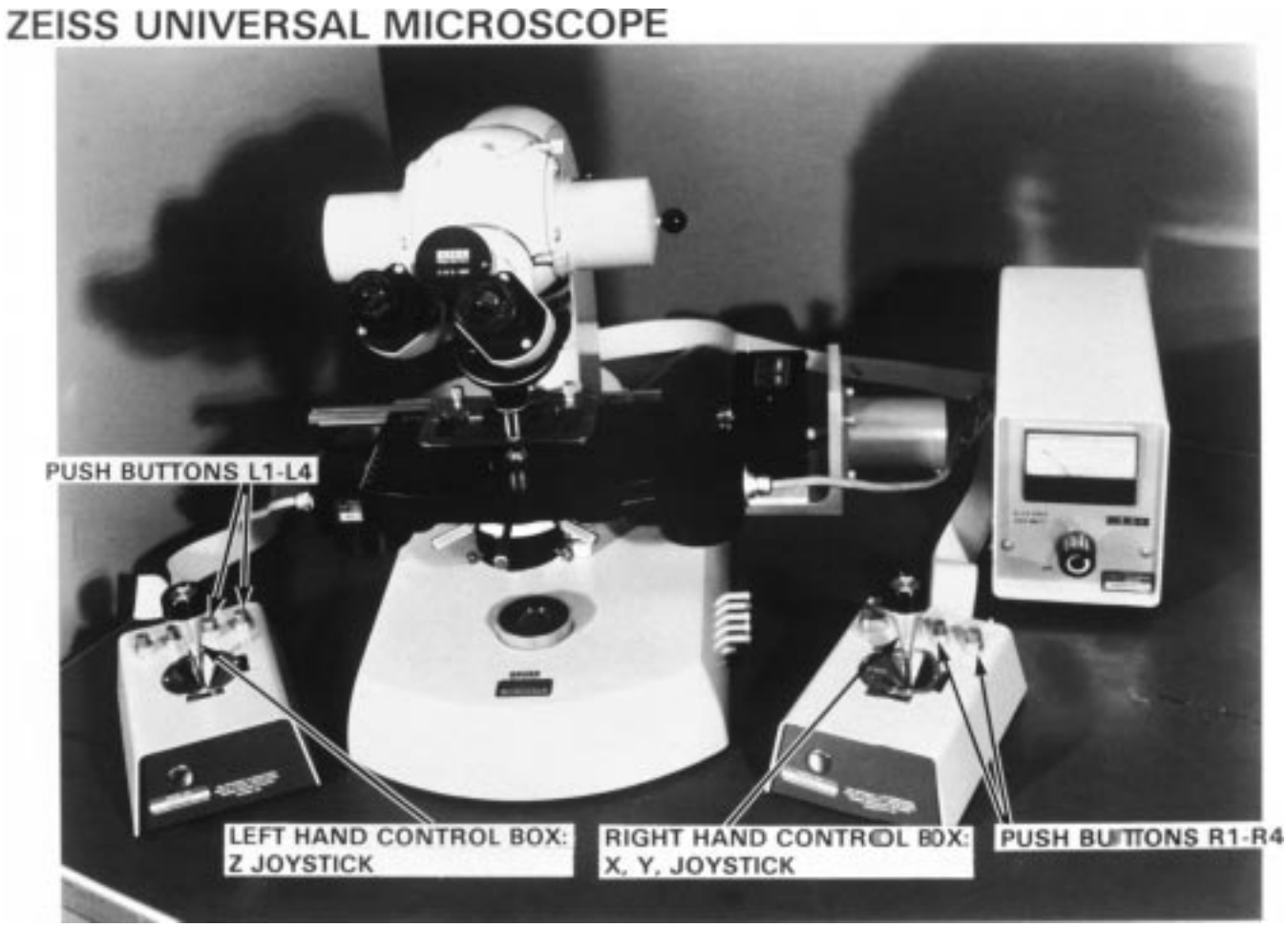

FIG. 8 Close Up of the ESP Microscope Showing Push Buttons and Stage Controls

TABLE 7 Push Button Controls

Push Button	Function/Operation
1L	*Store Data*—Use to store track data on disk if acceptable
2L	*No Storage*—Use to reject track data as unacceptable and return to the center of the field so that measurement can be repeated
3L	*Check Zero Reference*—Use to return to zero reference point, G = 0, R = 0, S = 0. This allows check of zero reference point for possible NRE misalignment.
4L	*Next Field/Stop Scanning*—Push to move to the next field for scanning or to stop scanning. Series of prompts must be answered to obtain the desired result.
1R	*Jog/Normal*—Allows fine motion control
2R	*Store Point*—Stores present location. Use to record points of a track, that is, the ends or breakpoints of a track.
3R	*Zero Reference*—Use to align reticle cross hair and push to set zero reference ($G = 0$, $R = 0$, $S = 0$).
4R	*Final Point/Restore*—Push after final track point has been stored. The computer automatically retraces the track and computes track length.

scanner can be examined.

9.3.5 *Track Selection*—The field is scanned by continuously increasing the S coordinate with the left joystick. The microscope focus is moved slowly downward in the NRE until one end of a track comes into focus. This track ending is moved until it is focussed at the center of the field under the reticle cross hair. By pressing push button 2R, the (*X,Y,Z*) coordinates of this track ending are recorded. The other end of the track is then brought into focus, provided the track is reasonably straight, and these (X,Y,Z) coordinates are recorded by pressing button 2R.

9.3.6 *Breakpoints*—If the track possesses breakpoints, where the recoil proton has been scattered, coordinates of these points are also recorded, so that the straight track segments can be added to give the track range. Hence, coordinates of the breakpoints are centered under the cross hair and stored as intermediate points of the track. This operation continues until the end of the track is reached, centered under the reticle cross hair and recorded as the final coordinates of the track. Actuation of push button 4R automatically retraces the track and displays the track length. If the observer is satisfied with the results, the track data can be stored on a scanning data disk by actuation of push button 1R. In terms of these observations, track length r is given by:

$$r = \left\{ \sum_{i=1}^{i=n} \left[\left(X_i - X_{i+1} \right)^2 + \left(Y_i - Y_{i+1} \right)^2 + h^2 \left(Z_i - Z_{i+1} \right)^2 \right] \right\}^{1/2} \quad (16)$$

Here (X_i, Y_i, Z_i) and (X_{i+1}, Y_{i+1}, Z_{i+1}) are consecutive track points. For a track possessing no breakpoints, obviously $n = 2$, whereas $n > 2$ for tracks possessing breakpoints. The scalar h accounts for shrinkage of the emulsion due to the NRE development process. Hence, h is given by the ratio of the

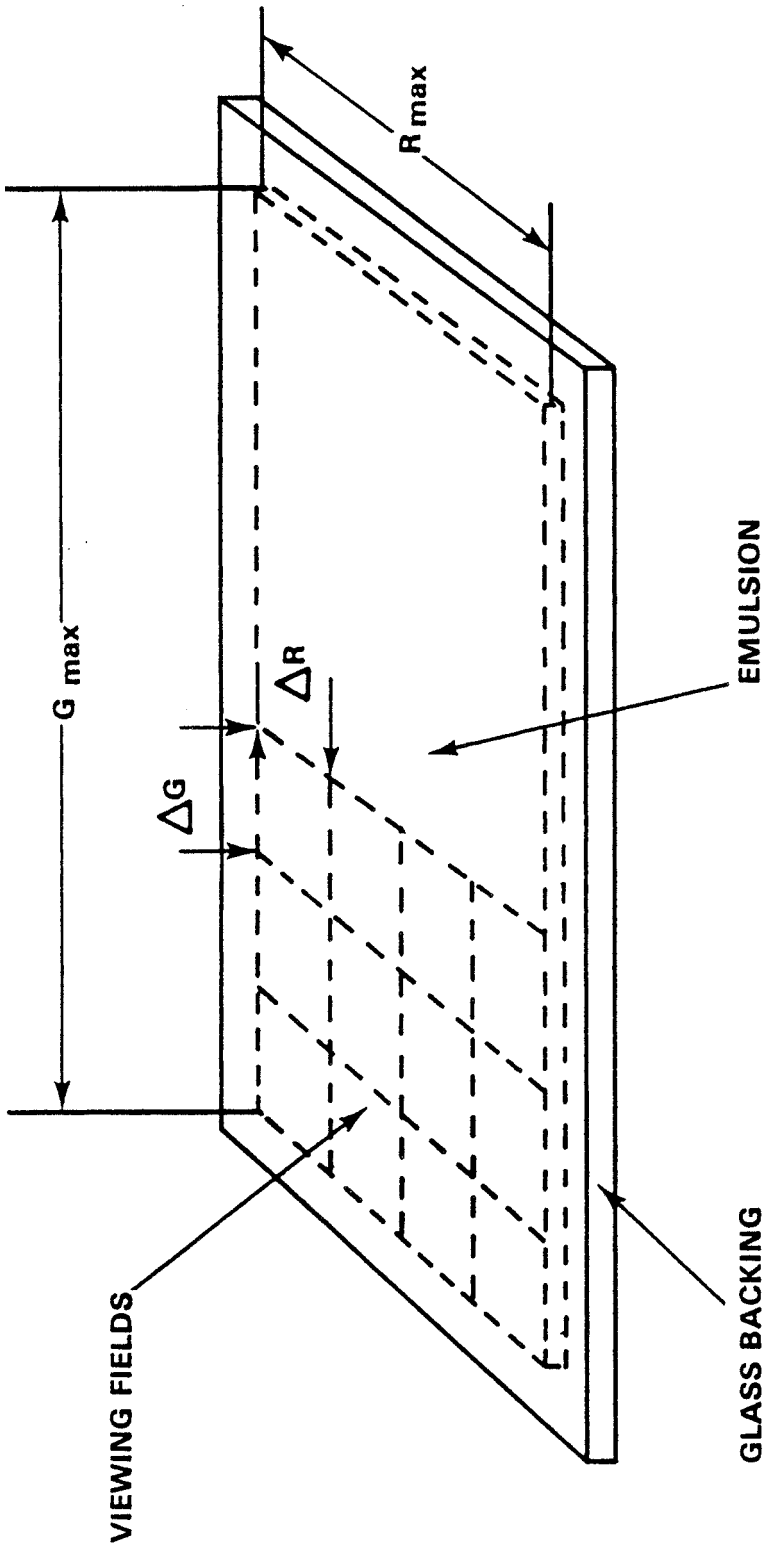

FIG. 9 Maximum Traverse Dimensions, G_{max} and R_{max}, Together with the Field Dimensions, ΔG and ΔR, Define the Number of NRE Scanning Fields Available for ESP Operation

emulsion thickness before development to the emulsion thickness after development, that is, $h = HO/HP$ (see Eq 14). Where immersion oil of the same refractive index as the emulsion gelatin is used, the measured displacement of the microscope objective will be equal to the difference in z coordinates. If a dry objective of large aperture is used, the z displacement of the objective should be related to the true difference between the z coordinates through calibration **(2)**.

9.3.7 *Track Acceptance Criteria*—If the track data is accepted, the system is returned to the S-level corresponding to the first observed track ending and the scanner then can continue to move down in S until one end of the next track is brought into focus, and the process is repeated. If the operator moves the cross hair outside the field volume being scanned, as defined by the current *G, R,* and S coordinates, then a warning tone will sound. As a consequence of this feature, only tracks that either begin or end in the field volume are scanned (see Fig. 7). In addition, if the observer attempts to measure a track that has already been stored, the warning tone also rings. This warning feature prevents duplicate track observations and, therefore, provides for more efficient NRE scanning.

9.3.8 *End-of-Field Condition*—Scanning proceeds by continuously increasing the S coordinate until a warning tone sounds, which indicates that the operator has exceeded the allowed S coordinate. Having reached the end of the field, the operator actuates push button 4L so that the computer can move the NRE to the next field to be scanned. The entire procedure is then repeated for this new field. Scanning thus continues until a sufficient number of tracks has been measured.

9.4 *End-On Mode Scanning*:

9.4.1 *Measurement of Scattering Angle*—In scanning end-on exposures with a computer based interactive system, the general operations described above are used together with supplemental procedures instituted in order to measure proton-recoil direction. The zero reference point is chosen by measuring a known distance from the mid-point of the leading edge with the microscope stage vernier G and R scales. At these selected vernier settings, a proton track escaping from the top surface is chosen and the zero reference point is the point of escape of this track. After entering the initial (*X, Y, Z*) coordinates of a track, the direction of the track is measured by entering an intermediate point on the track. For a valid direction measurement when the track possesses breakpoints (where the recoil-proton has been scattered), the intermediate point must be chosen in the track segment between the initial track point and the first breakpoint. For end-on mode scanning, one normally stays quite close to the leading edge of the NRE ($\leq$ 1 mm) in order to render neutron multiple scattering effects negligible.

9.4.2 *Effective Cross Section*—In order to determine the partial σ_{np} (E) cross section used in the end-on mode observations, which provides the energy dependent emulsion efficiency, scanning must be carried out in a known solid angle. Hence, only tracks that lie in a preselected scattering angle interval: $0 \leq \theta \leq \theta_{max}$ are accepted. After the intermediate point is entered, the angle θ is automatically calculated and a tone sounds if θ does not lie in this preselected interval. Consequently, when θ does not satisfy this prescribed condition, the track data are rejected and the system automatically returns to the center of the current (G_kR_j) field (at the same S-level) so that scanning can continue.

10. Experimental Uncertainties in NRE Measurements

10.1 *Systematic Uncertainties*—Sources of systematic uncertainty for absolute NRE neutron spectrometry are summarized in Table 8. In this table, the first four uncertainty sources have already been quantified by earlier efforts **(3-6)**. The fifth source of systematic uncertainty, namely volume measurement uncertainty, is discussed in section 10.1.1 below. Since these systematic uncertainties are independent, the quadrature uncertainty for all systematic effects in NRE neutron dosimetry comes to approximately 5 %.

10.1.1 *Volume Measurement Uncertainty*—The volume of emulsion scanned is an important observable in absolute neutron measurements, where absolute proton-recoil energy spectra or reaction rates are required per hydrogen nucleus or equivalently per unit volume of emulsion scanned. A relative uncertainty of 2 % (1σ) for volume measurements can be determined by mounting a stage micrometer in the scanning system. This uncertainty estimate stems mainly from nonlinearity of the electromechanical motion over the range of travel in the G, R, and S directions. Actually, this 2 % (1σ) estimate is conservative, since it represents the uncertainty arising in small volume measurements corresponding to, at most, a few fields of view. For larger volume measurements, over an extended number of fields, cancellation of errors in the electromechanical stepping components of the interactive system produces a significant reduction in uncertainty. Since this uncertainty estimate was obtained with the ESP system, one would expect a smaller uncertainty value for an interactive system fabricated with current state-of-the-art components.

10.2 *Random Uncertainties*

10.2.1 *Track Counting Uncertainty*—The applicability of Poisson statistics for describing random uncertainty in track counting was established some time ago **(21)**. Consequently, the standard deviation[5] associated with the observation of N tracks is given by $\sigma_N = (N)^{1/2}$.

10.2.2 *Range Measurement Uncertainty*—Uncertainty in range measurements can be determined by comparing results obtained by different observers. Comparisons on the ESP system were carried out in two different ways, namely with a rescan method and a preselected set method **(17)**. In the rescan method, observers randomly selected fields that had already

[5] The standard deviation of x is denoted by σ_x and the variance of x is denoted by σ_x^2.

TABLE 8 Systematic Uncertainty Estimates for Absolute Neutron Dosimetry with NRE

Source of Uncertainty	Relative Uncertainty, % (1σ)
Proton Range Straggling	2
Proton Range-Energy Relation	2
NRE Hydrogen Density	3
Hydrogen Cross Section, σ_{np}	1
Volume of NRE Scanned	2

TABLE 9 Random Uncertainty Estimates for Absolute Neutron Dosimetry with NRE

Source of Uncertainty	Uncertainty (1σ)
Track Counting Statistics	$(N)^{1/2A}$
Proton Range Measurements	0.52μ

[A]Standard deviation of *N* observed tracks assuming a Poisson track counting probability distribution.

been scanned by other observers. In the preselected set method, a set of tracks was chosen and all observers scanned this set. Both methods produced essentially the same result, namely a standard deviation of ~0.52 micron for the range measurement uncertainty. As an example, Fig. 10 presents the relative frequency histograms for $|\Delta X|$, $|\Delta Y|$, $|\Delta Z|$ and Δr obtained using the rescan method on the ESP system. The average value obtained from each of these frequency histograms represents an estimate of the standard deviation in ESP measurements of each respective observable. These histograms yield estimates of 0.38, 0.36, 0.51 and 0.52 μm for σ_x, σ_y, σ_z *and* σ_R, *respectively.*

10.3 *Treatment of Random Uncertainties*—Integral measurements from two NRE irradiated in the PCA benchmark field will be used to illustrate the treatment of random uncertainties. Integral mode scanning of these two NRE with the ESP system concentrated on the range region between 4 and 8μ, which corresponds to the energy region from 0.407 to 0.682 MeV. These observations are presented in Figs. 11 and 12. The data shown in Figs. 11 and 12 were obtained by partitioning the 4 to 8μ region into 1μ intervals, so that $M(R_i)$ is the observed number of tracks in the interval from $(R_i - 0.5\mu)$ to $(R_i + 0.5\mu)$. Hence on the basis of Possion statistics, the standard deviation of M_i is given by $\sigma_{Mi} = (M_i)^{1/2}$.

10.3.1 Using this uncertainty estimate together with the data points $\{R_i, M(R_i)\}$, a linear least squares fit of the observed proton-recoil data was obtained in the form:

$$M(R) = a + b \cdot R \tag{17}$$

where: *a* and *b* are the intercept and slope, respectively, as determined by the least squares analysis. As can be seen in Figs. 11 and 12, this linear assumption provides an excellent description of the data observed in both NRE. An attempt was made to optimize the linear least squares fit by changing the partitioning of the data to 0.5μ intervals. It was found that the linear least squares fit was quite insensitive to whether four points (tracks/micron) or eight points (tracks/0.5 micron) were used in this range interval.

10.3.2 *I Integral Random Uncertainty*—To obtain uncertainty estimates for *M(R)* that accounts for both Poisson fluctuations as well as the uncertainty in range measurements, this linear least squares analysis must be repeated with input uncertainties given by:

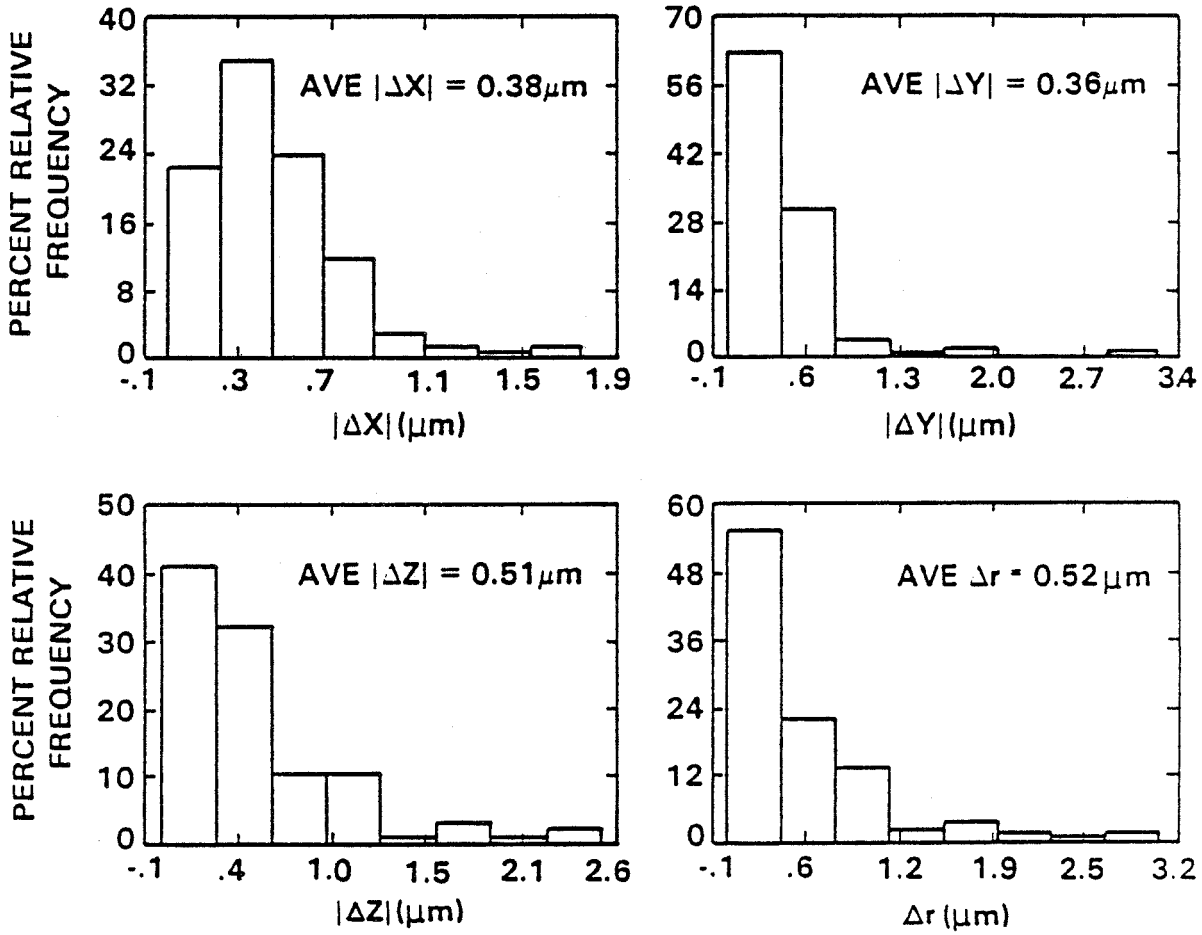

FIG. 10 Relative Frequency Histograms for |ΔX|, |ΔY|, |ΔZ| and |ΔR| Obtained Using the Rescan Method

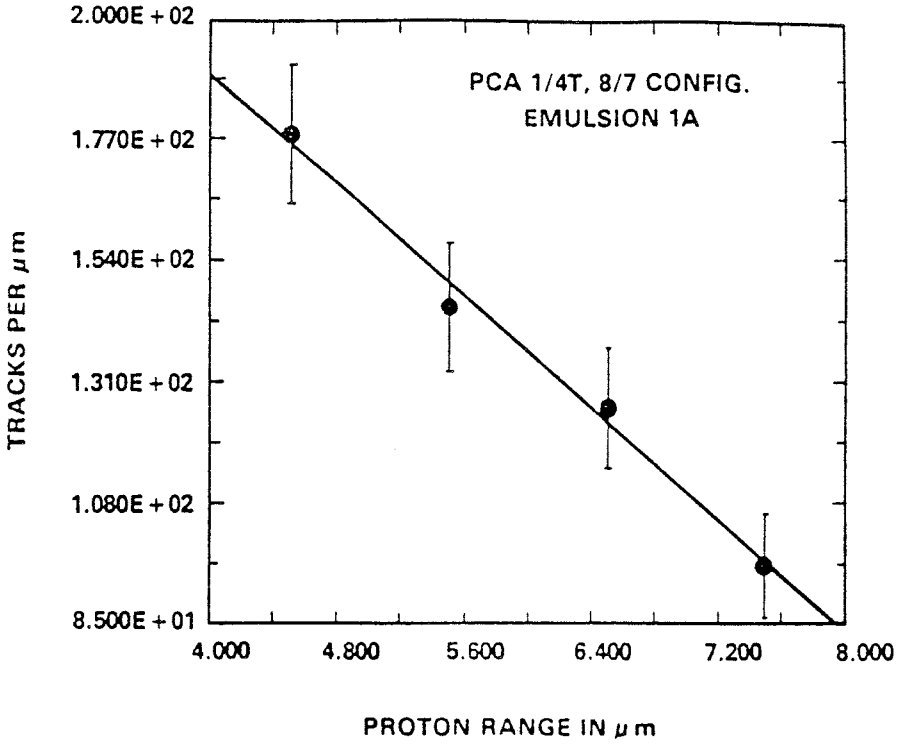

FIG. 11 Linear Least Squares Fit of the Range Data Observed in PCA NRE 1A Irradiated at the T/4 Location of the 8/7 Configuration

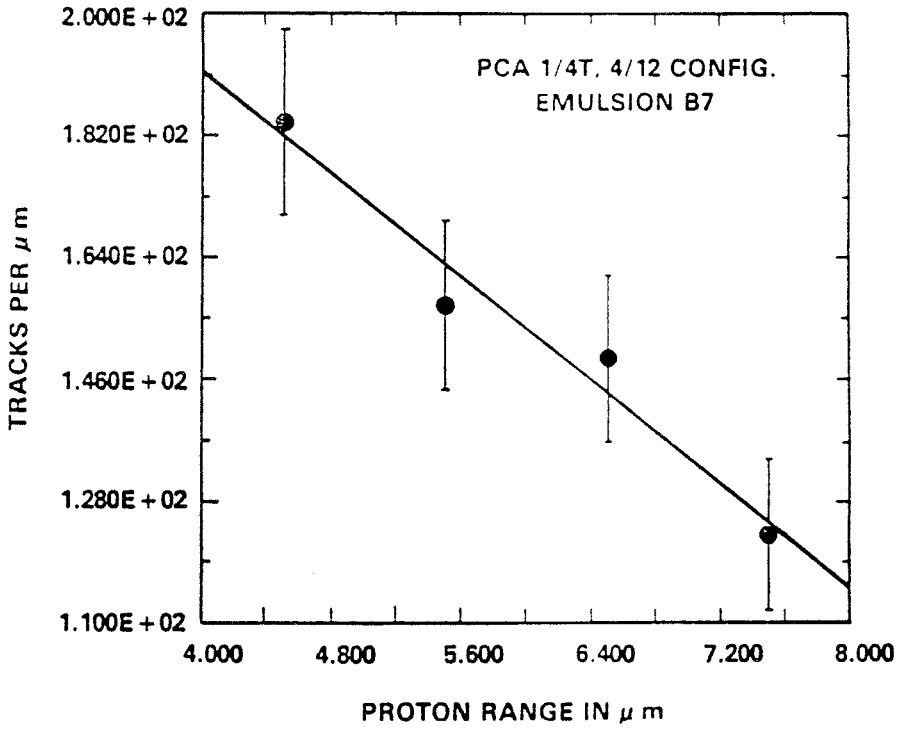

FIG. 12 Linear Least Squares Fit of the Range Data Observed in PCA NRE B7 Irradiated at the T/4 Location of the 4/12 SSC Configuration

$$\sigma_{M_i}^2 = M_i + b^2 \cdot \sigma_R^2 \quad (18)$$

Here: b is the slope obtained from the first linear least squares fit and as before σ_R is the standard deviation in range measurements determined with the (ESP) interactive scanning system. These new values of uncertainty together with the data points { R_i, $M(R_i)$ } are used as input data for the second linear least squares analysis of the form given by Eq 17. This second least squares analysis provides a variance-covarriance matrix,

VCM, which can be used to calculate the uncertainty in the linear representation of *M(R)*. VCM can be expressed in the form:

$$VCM = \begin{pmatrix} \sigma_a^2 & \sigma_{ab} \\ \sigma_{ab} & \sigma_b^2 \end{pmatrix} \quad (19)$$

and this matrix form can be used to calculate the uncertainty of the linear representation of M(R). Using Eq 17 and 19, one finds

$$\sigma_{M_i}^2 = \sigma_a^2 + 2\sigma_{ab} R + \sigma_b^2 R^2 \quad (20)$$

10.3.3 *J Integral Random Uncertainty*—The random uncertainty in $\mu_i(R)$ is given by:

$$\sigma_{\mu i}^2 = \mu_i + M_i^2 \cdot \sigma_R^2 \quad (21)$$

The first term on the right hand side of Eq 21 represents the random uncertainty that arises in the observation of the integral number of tracks, which is given by Poisson statistics. The second term on the right hand side of Eq 21 is the contribution due to the random uncertainty in range measurements, which follows from Eq 12.

10.4 *Total Uncertainty of NRE Integral Dosimetry*—Total uncertainties for NRE integral dosimetry can be obtained by combining uncertainty components that are described in sections 10.1, 10.2 and 10.3. As a result, the typical uncertainties for I integral measurements fall in the range from approximately 7 to 10 % (1σ), whereas the typical uncertainty of J integral measurements is approximately 6 % (1σ).

10.5 *Additional Sources of Uncertainty*—The above considerations have been restricted to uncertainties that arise in the NRE experimental technique. Additional uncertainties arise from the in-situ reactor irradiations, such as uncertainty in the exposure time t and the need to scale to the absolute power of the benchmark field. These two additional components of experimental uncertainty will vary for different benchmark fields. NRE experiments in LWR-PV benchmark fields reveal that each of these two additional components of uncertainty are typically a few percent (1σ).

11. Attributes of NRE for In-Situ Integral Neutron Dosimetry

11.1 *Comparison of NRE and Active Proton-Recoil Methods*—As has already been stressed, no single method of reactor neutron spectrometry exists which can completely cover the energy range of interest in reactor environments **(12)**. The best energy resolution and counting statistics can be obtained using proton-recoil proportional counters (PRPC) filled with hydrogen or methane. However, proton escape from the sensitive volume of small in-situ proportional counters creates a high energy limitation for PRPC neutron spectrometry. Moreover, ionization induced by proton-recoil events in PRPC produces electronic signals, which are processed by suitable on-line instrumentation and computers. However, all information related to proton-recoil direction and spatial energy deposition is lost. This deficiency makes correction of proton escape much more difficult for PRPC, where corrections for finite size effects become non-negligible above approximately 0.5 MeV **(13)**. Fortunately, the NRE neutron dosimetry method complements PRPC neutron spectrometry. Because proton-recoil range is much shorter in NRE than PRPC, finite size effects are significantly less in NRE. Of perhaps equal importance is the fact that analytical correction of proton-recoil escape from NRE is much more tractable than for PRPC.

11.2 *Perturbation Effects*—The I and J integral reaction rates can also be derived from active proton-recoil neutron spectrometry, whether employing PRPC or liquid/plastic scintillators. I and J integral reactions rates based on these active methods possess two distinct disadvantages in comparison to NRE integral reaction rates. NRE experiments in VENUS-1 demonstrated that PRPC create a significant perturbation of the neutron field found in LWR-PV environments **(20)**. Perturbation factors for the I and J integral behaved differently, with the I integral perturbation factors varying from approximately 0.74 up to 1.44, whereas the J integral perturbation factor varied from approximately 1.0 up to 1.41. These observations also revealed that proportional counter perturbation factors depend in a complex way on in-situ spatial location and environment as well as neutron energy. Perturbation factors for liquid or plastic proton recoil scintillators can be expected to be as large and vary as complexly as those of PRPC, since these scintillation detectors are invariably larger in size.

11.3 *Finite-Size Effects*—The second disadvantage of these active spectrometry methods arises from the need to correct proton recoil spectra for the escape of proton recoil events from the active volume of the detector. Simple geometrical analysis can be used to treat proton-recoil escape from the active volume of the NRE **(14,15)**. In contrast, finite-size effects for PRPC are considerably more difficult to treat. Active detectors do not reveal (on an event-by-event basis) whether or not escape has occurred for each observed proton recoil event. One must generally resort to characterizing the active detector response function and correct the observed proton recoil spectrum through an unfolding calculation **(13)**. As a consequence, finite-size effects can be corrected much more accurately for NRE observations than is possible for active detector measurements. As an example, Fig. 13 compares finite size correction factors for PRPC and NRE. The uncertainty in neutron fluence introduced by correction of finite size effects in NRE is shown in Fig. 14. Since integral NRE neutron dosimetry in benchmark fields usually covers the energy range from approximately 0.4 up to 1.0 MeV, these two figures reveal that finite size effects can be ignored in NRE integral neutron dosimetry.

12. Keywords

12.1 fast-neutron dosimetry; NRE; nuclear emulsions; optical microscopes; proton-recoil tracks

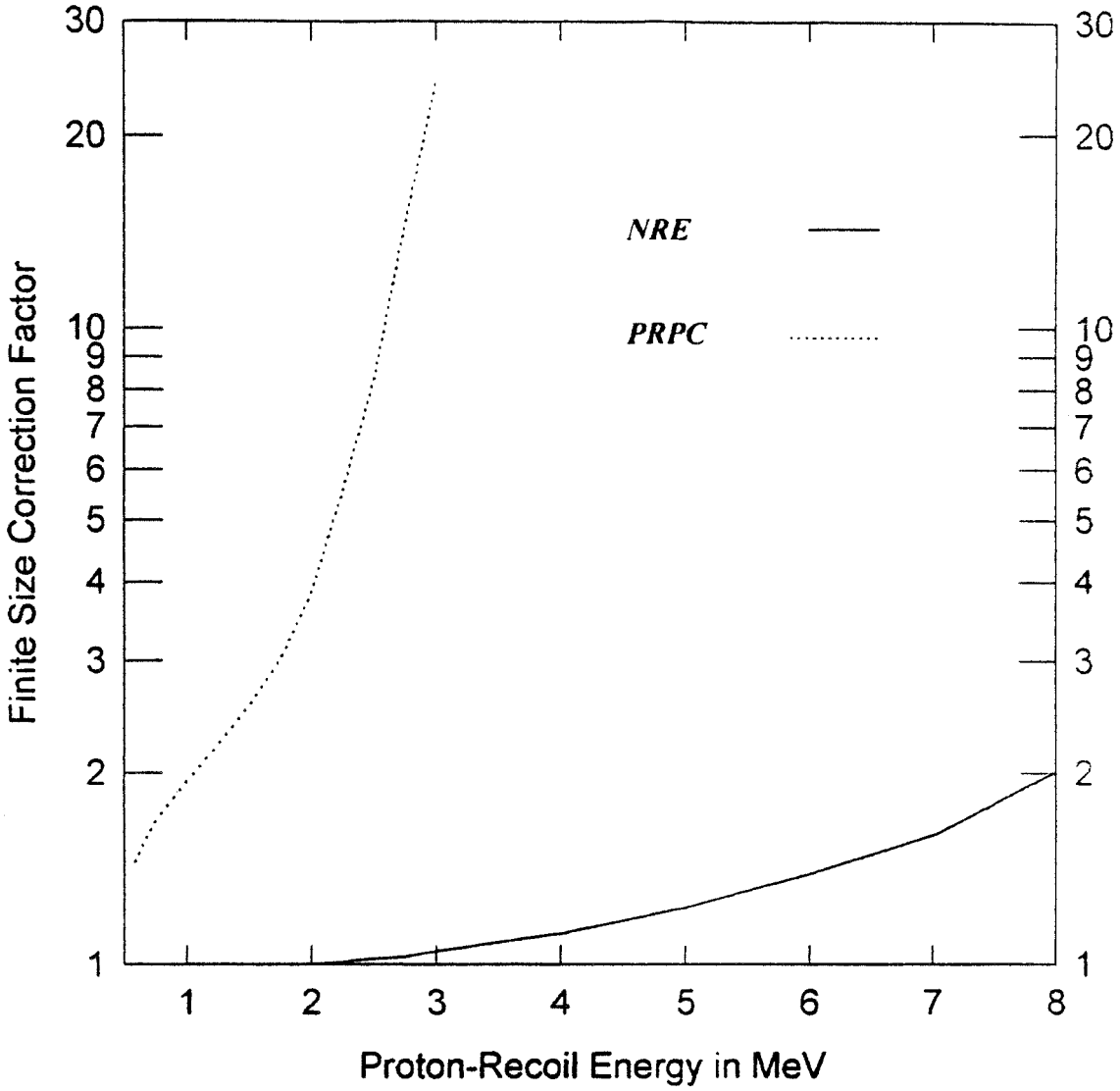

FIG. 13 Finite Size Correction Factors for NRE and PRPC as a Function of Proton-Recoil Energy

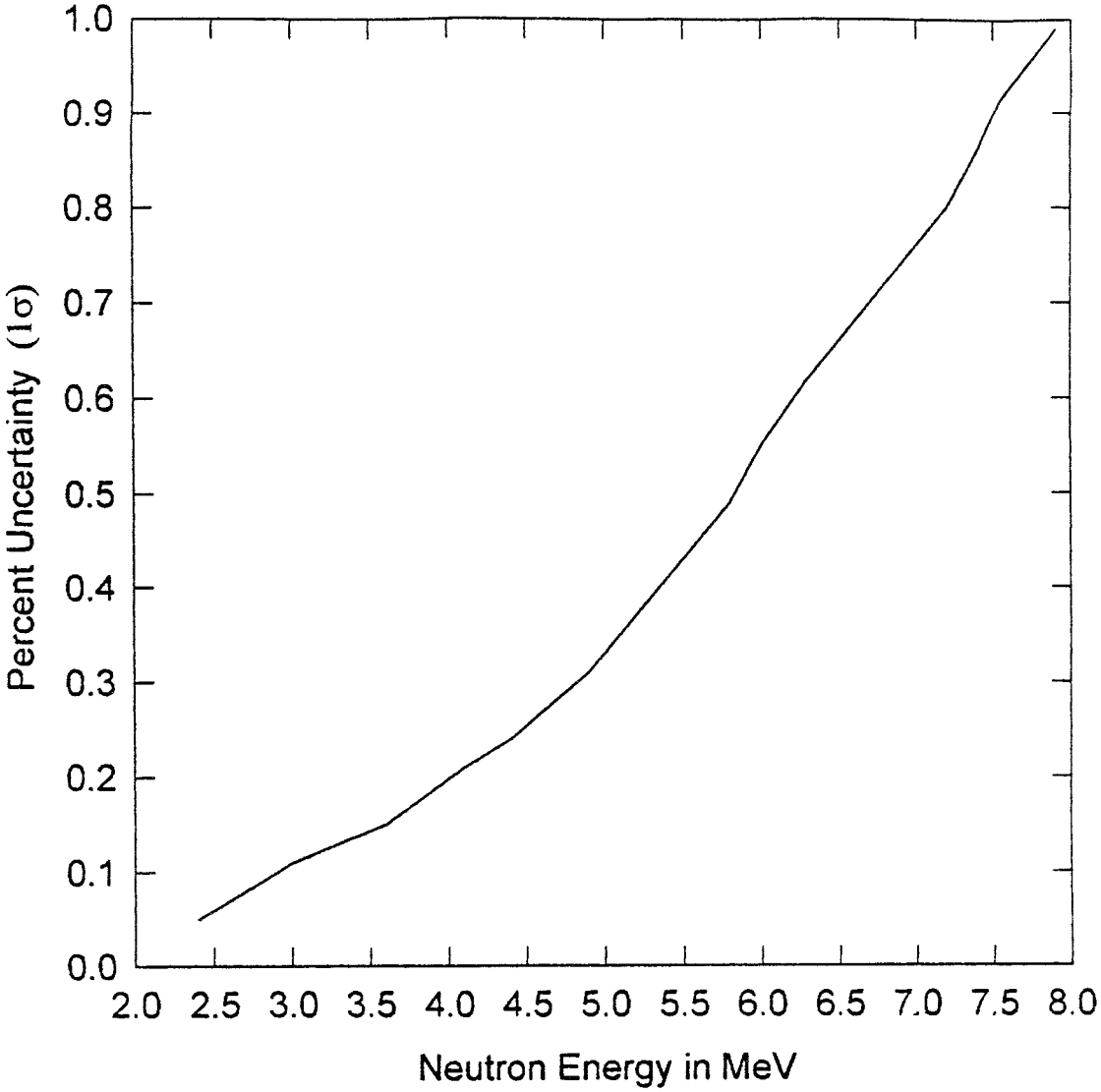

FIG. 14 Uncertainty Introduced into Neutron Fluence by Finite Size Correction for Proton-Recoil Escape from a 400μ NRE

REFERENCES

(**1**) Powell, C. F., Fowler, F. H. and Perkins, D. H., *The Study of Elementary Particles by the Photographic Method*, Pergamon, New York, 1959.

(**2**) Barkas, W. H., *Nuclear Research Emulsions*, Vol. I, Academic Press, New York, 1963.

(**3**) Rosen, L. "Nuclear Emulsion Techniques for the Measurement of Neutron Energy Spectra," Nucleonics 11, 1953 and 12, 1953.

(**4**) Roberts, J. H. "Absolute Flux Measurements of Anisotropic Neutron Spectra with Proton Recoil Tracks in Nuclear Emulsions," *Rev. Sci. Instr. 8*, 1957.

(**5**) Roberts, J. H. and Behkami, A. N. "Measurements of Anisotropic Neutron Spectra with Nuclear Emulsion Techniques," *Nucl. Appl. 4*, 1968.

(**6**) Barkas, W. H., *Nuclear Research Emulsions*, Vol. II, Chapter 6, Neutron Measurements, Academic Press, New York, 1973.

(**7**) Roberts, J. H., Gold, R., Preston, C. C., Hendricks, C. A., McNeece, J. P. and Ruddy, F. H., "Neutron Spectrometry in the Fast Test Reactor with Nuclear Research Emulsions: Observation of Angular Anisotropy," HEDL-TC-1977 Addendum, August 1981.

(**8**) Keepin, G. R. and Roberts, J. H., "On the Measurement of the Energy of Fast Neutrons by Photographic Emulsion Loaded with Enriched ^{6}Li," Phys. Rev. 28, 1957, pp. 610–615.

(**9**) Frye, G. M. and Gammell, J. H., "^{10}B(n,t2α) and ^{10}B(n,dn′2α) Reactions for 6-20 MeV Neutrons," *Phys. Rev. 103, 328*, 1956.

(**10**) Gold, R., Roberts, J. H., Ruddy, F. H., Preston, C. C. and Hendricks, C. A., "Proton-Recoil Emulsion Observations for Integral Neutron Dosimetry," Proc. of the IAEA Advisory Group Meeting on Nuclear Data for Radiation Damage Assessment and Related Safety Aspects, Vienna, October 12-18, 1981, IAEA-TECDOC-263, International Atomic Energy Agency, Vienna, Austria, 1982, pp. 115–121.

(**11**) Roberts, J. H., Gold, R., Ruddy, F. H., Preston, C. C. and McNeece, J. P., "Fast Neutron Fluence-Spectra and Integral Reaction Rates Determined with Nuclear Research Emulsions," *12th International Conference on Solid State Nuclear Track Detectors*, Acapulco, Mexico, 4-10 September, 1983.

(**12**) Gold, R. "Neutron Spectrometry for Reactor Applications: Status,

Limitations, and Future Directions," *First International ASTM-EURATOM Symposium on Reactor Dosimetry*, Petten, 1975, Part I, 119, EUR-5667, 1977.

(**13**) Gold, R. and Bennett, E. F., "Effects of Finite Size in 4π-Recoil Proportional Counters," *Nucl. Instr. and Methods*, 1968, pp. 285-299.

(**14**) Gold, R. and Roberts, J. H., "Nuclear Emulsion Neutron Spectrometry in the FFTF," *Trans. Am. Nucl. Soc. 34*, 146, 1980.

(**15**) Gold, R., Roberts, J. H., Preston, C. C., Hendricks, C. A., McNeece, J. P. and Ruddy, F. H., "Neutron Spectrometry in the Fast Test Reactor with Nuclear Research Emulsions," HEDL-TC-1977, August 1981.

(**16**) Lippincott, E. L. and McElroy, W. N. *FTR Dosimetry Handbook*, HEDL MG-166, Hanford Engineering Development Laboratory, Richland, WA, 1983.

(**17**) Gold, R., Roberts, J. H., Preston, C. C., Ruddy, F. H., Cooper, C. S., Hendricks, C. A., Johnson, D. T., McNeece, J. P., Main, G. W., Michaels, T. E., Spence, N. E. Svoboda, H. J. and Vargo, G. F. Jr., "Interactive System for Scanning Tracks in Nuclear Research Emulsions," *Rev. Sci. Instrum.* 54, 1983, pp. 183-192.

(**18**) Roberts, J. H., Gold, R. and Preston, C.C. "Measurements Of The Absolute Fluence Spectrum Emitted At 0° and 90° From The Little-Boy Replica," 13th International Conference on Solid State Nuclear Track Detectors, Rome, 22-27 September, 1985, *Nucl. Tracks and Radiation Measurements 12*, 553, 1986.

(**19**) Gammell, J. L., *Fast Neutron Physics*, Part II, J. B. Marion and J. L. Fowler, Eds., Part II, Wiley (Interscience), New York, NY, 1961

(**20**) Gold, R., Preston, C. C., Roberts, J. H., DeLeeuw, G., Fabry, A. and Leenders, L.," Nuclear Research Emulsion Measurements and the Observation of Proportional Counter Perturbation Factors in VENUS-1," *Proc. 6th ASTM-EURATOM Symposium on Reactor Dosimetry*, Jackson Hole, Wyoming, May 31-June 6, 1987, *ASTM STP 1001*, 1989, pp. 348-356.

(**21**) Gold, R., Roberts, J. H. and Armani, R. J. "Absolute Fission Rate Measurements with Solid-State Track Recorders," *Nucl. Sci. Eng. 34*, 13, 1968.